

Supporting Information for

Direct Visualization of Photomorphic Reaction Dynamics of Plasmonic Nanoparticles in Liquid by Four-Dimensional Electron Microscopy

Xuewen Fu,^{*,†} Bin Chen,[†] Caizhen Li,[‡] Heng Li,[†] Zhi-Min Liao,^{*,‡} Dapeng Yu,[§] Ahmed H. Zewail^{†,||}

[†]Physical Biology Center for Ultrafast Science and Technology, Arthur Amos Noyes Laboratory of Chemical Physics, California Institute of Technology, Pasadena, California 91125, United States

[‡]State Key Laboratory for Mesoscopic Physics, School of Physics, Peking University, Beijing 100871, China

[§]Institute for Quantum Science and Technology and Department of Physics, South University of Science and Technology of China (SUSTech), Shenzhen 518055, China

*E-mail: xfu@bnl.gov;

*E-mail: liaozm@pku.edu.cn.

||Deceased.

This PDF file includes:

Materials and Methods; Supporting Figure S1; Captions for Movies S1 to S5.

Other supplementary information for this manuscript includes the following:

Movies S1 to S5

Materials and Methods

Preparation of liquid cell

For the preparation of liquid cell in this work, standard TEM silicon nitride windows ($50\ \mu\text{m} \times 50\ \mu\text{m}$) on 200- μm -thick silicon frame with a thin gold film of about $\sim 200\ \text{nm}$ without blocking the window deposited by thermal evaporation as a spacer were used (customized from Norcada Inc.). The ultrathin low-stress silicon nitride membrane is approximately $20\ \text{nm}$ in the thickness, deposited by low-pressure chemical vapor deposition, which guarantees the spatial resolution of the liquid cell to be in nanometer range. The preparation of liquid cells is given as follows. The silicon nitride membrane was firstly rinsed with acetone, isopropyl alcohol, and deionized water followed by plasma cleaning ($P \sim 3.5\ \text{W}$) for $30\ \text{s}$. The plasma cleaning makes the silicon nitride membrane hydrophilic to aqueous solution. Then a drop of $\sim 5\ \mu\text{L}$ aqueous solution with gold nanoparticles (AuNPs, capped by negatively charged citrate) with diameter of $60\ \text{nm}$ (Nanocomposix Inc.) was loaded on the bottom chip, and another chip without spacer was put on the surface of the liquid. Because of the surface tension of the liquid, the top silicon nitride window would rotate freely and align well with that of the bottom one. These two well-aligned silicon nitride window chips were then clamped by a tweezer, and the superfluous liquid was absorbed by a small piece of filter paper from the side. Thus, a thin layer of liquid was sandwiched between the two chips with the thickness equivalent to the spacer thickness. Finally, an epoxy (Ted Pella Inc.) was used to seal the side of the liquid cell. After the sealing was dried, the liquid cell was loaded in our 4D-EM for measurements. During the experiment, we checked each liquid cell sample by tilting it to different view angles and excluded the bad one with gas bubbles or without liquid or with apparent bulges of the window.

Time-resolved imaging in liquid

The measurements were performed in our 4D-EM instrument (UEM-1 at Caltech) with the integration of liquid cell. fs-infrared laser pulses (1040 nm, 350 fs FWHM pulse duration) were used to generate the visible pump fs-laser pulses (520 nm) via second harmonic generation and the green fs-pulses were directed to the liquid cell sample inside the microscope to trigger the dynamics. Precisely synchronized UV ns-laser pulses (266 nm, 10 ns FWHM pulse duration) were directed to the photocathode inside the TEM to generate ns-electron pulses, which were accelerated to 120 keV to probe the dynamics by transient imaging. The synchronization between the ns probe pulse and the fs pump pulse was achieved by a digital delay generator. For the time-resolved imaging measurement at long times, namely, continuous-pulse imaging mode, the sample was excited by 1 kHz green fs-laser pulses, and a continuous e-beam with a low electron dose were continuously presented to take a video to capture the dynamics. The frame rate of the video is 10 frames per second, and the exposure time for each frame is ~0.1 second. While for the time-resolved imaging measurement at short time scale, i.e. single-pulse-imaging mode, a single green fs-laser pulse was used to trigger the dynamics and a precisely timed ns-electron pulse was used to image the consequent transient dynamics at a specific delay. The time resolution of our 4D-EM instrument is ~10 ns.

PINEM measurement

The PIENM measurements were carried out in UEM-2 at Caltech, which is a modified TEM equipped with a high power fs-laser system.¹⁻² Compared with UEM-1 system, in addition to the different high power fs-laser, UEM-2 system was equipped with an electron energy filter for electron energy spectrum measurement. The synchronous excitation and probing of sample was achieved by overlapping the fs-electron and fs-photon pulses on the sample, both in space and time. The wavelength of the optical excitation pulse was 520 nm ($\hbar\omega = 2.4$ eV), and its FWHM pulse duration

was 220 fs. The probing fs-electron pulse was generated by 260 nm fs-laser pulse (obtained by second harmonic generation of the 520 nm fs-laser pulse) excitation on the photocathode in the electron microscope, and was accelerated to 200 keV. The temporal synchronization and delay control of these two pulses were achieved by using an optical delay line in an interferometry arrangement. The time zero was determined when the maximum of the inelastic scattering peaks in PINEM was obtained. The repetition rate of the optical laser pulse was typically at 500 kHz, and the linearly polarized laser beam was focused to $\sim 40 \mu\text{m}$ diameter area on the sample.

Estimation of transient temperature in the AuNPs with fs-laser pulse excitation

Since the silicon-nitride and water is almost transparent to the excitation laser wavelength used in our experiment, upon the fs-laser pulse excitation the optical pulse energy is firstly absorbed by the AuNPs through the strong optical absorption by localized surface plasmon enhancement, resulting in a rapid rise of the electron temperature and subsequently equilibrating with the lattice in tens of picoseconds through electron-phonon couplings.² This results in a nonequilibrium temperature of the AuNPs and the thermal energy in the AuNPs subsequently dissipates to the surroundings. With a fs-laser pulse excitation, the transient thermal state of the AuNPs can be described by a two-temperature model,³

$$C_e \frac{dT_e}{dt} = g(T_l - T_e) + \frac{E_{\text{abs}}}{V_p \cdot \tau_{\text{pulse}}}, \quad (1)$$

$$C_l \frac{dT_l}{dt} = g(T_e - T_l) - \frac{\dot{Q}_w}{V_p} \quad \text{if } T_l < T_m. \quad (2)$$

Here V_p is the volume of the AuNP, τ_{pulse} is the laser pulse duration, T_e and T_l are the electron and lattice temperatures of the particle, E_{abs} is the laser pulse energy absorbed by the AuNP, g is the

coupling factor to calculate the heat transfer rate from electrons to the lattice, \dot{Q}_w is the rate of heat loss from AuNP to its surroundings, C_e and C_l are the heat capacities for the electrons and the lattice of bulk gold, respectively. T_m is the melting temperature of gold ($T_m \sim 1337$ K).³

The laser energy absorbed by the AuNP depends on the laser fluence, F_{pulse} , and the absorption cross-sectional area of the AuNP, A_{abs} , which is given by

$$E_{\text{abs}} = A_{\text{abs}} \cdot F_{\text{pulse}}. \quad (3)$$

The rate of heat loss from the AuNP to its surroundings in equation (2) is calculated by taking into account the interface thermal conductance given by

$$\dot{Q}_w = A_{\text{surface}} \cdot G \cdot (T_l - T_{w,s}), \quad (4)$$

where $T_{w,s}$ is the water temperature at the particle surface, G is the thermal conductance at the AuNP /fluid interface and A_{surface} is the surface area of the AuNP.

For the fs-laser pulse excitation, a pulsed wave can be used to characterize the temporal profile of the laser pulse. It is worth to note that the choice of temporal profile has no considerable effect on lattice temperature in the case of fs-laser excitation (~ 350 fs in our experiment) because the electron-phonon coupling time, on the order of tens of picoseconds,² is much larger than the pulse duration. A Gaussian temporal profile was used for the fs-laser pulse in our experiment. All the parameters used in the calculation were taken from Ref. 3. Using the above two-temperature model, the nonequilibrium maximum temperature of the AuNP can be estimated under a certain laser fluence below the melting threshold of the AuNP, for instance, the transient nonequilibrium temperature of the AuNPs is 750 ~ 800 K under the laser fluence of about 7.7 mJ/cm².

Supporting Figure S1

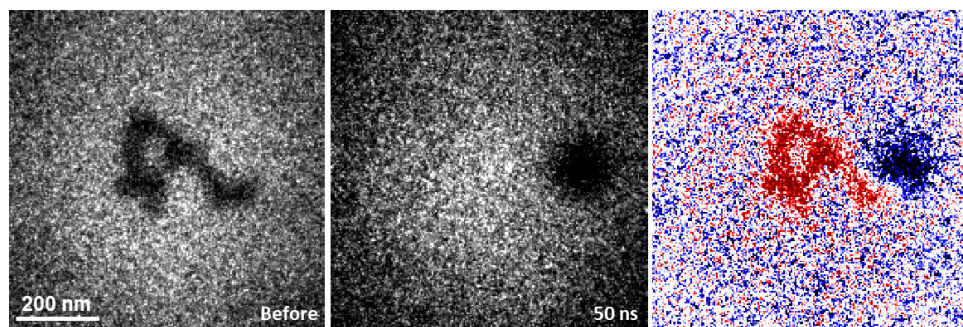


Figure S1. Single-pulse electron imaging result of several AuNPs fusion dynamics at ns time scale (fluence of 33 mJ/cm^2). (First column) Single-pulse image of the AuNPs in liquid cell before exposure to the laser pulse excitation. (Middle column) Single-pulse image of the AuNPs at 50 ns after the fs-laser pulse excitation. (Last column) The difference image obtained by subtracting the single-pulse image before the fs-laser pulse excitation from that at the short delay. Negative and positive contrasts are indicated by blue and red, respectively.

Captions for Movies S1 to S13

Movie S1. 1 kHz fs-laser pulse induced continue aggregation of AuNPs in liquid cell at a fluence of 3.3 mJ/cm^2 .

Movie S2. 1 kHz fs-laser pulse induced continue aggregation of AuNPs in liquid cell at a fluence of 2.0 mJ/cm^2 .

Movie S3. 1 kHz fs-laser pulse induced continue aggregation of AuNPs in liquid cell at a fluence of 4.9 mJ/cm^2 .

Movie S4. 1 kHz fs-laser pulse induced continue aggregation of AuNPs in liquid cell at a fluence of 7.7 mJ/cm^2 .

Movie S5. Continuous electron imaging of AuNPs agglomeration and fusion process under intensive laser pulse excitation shot by shot at a fluence of 33 mJ/cm^2 .

References:

1. Barwick, B.; Flannigan, D. J.; Zewail, A. H., Photon-induced near-field electron microscopy. *Nature* **2009**, *462* (7275), 902-906.
2. Barwick, B.; Park, H. S.; Kwon, O.-H.; Baskin, J. S.; Zewail, A. H., 4D imaging of transient structures and morphologies in ultrafast electron microscopy. *Science* **2008**, *322* (5905), 1227-1231.
3. Ekici, O.; Harrison, R.K.; Durr, N.J.; Eversole, D.S.; Lee, M. Ben-Yakar, A., Thermal analysis of gold nanorods heated with femtosecond laser pulses. *J. Phys. D: Appl. Phys.* **2008**, *41*(18), 185501.